Molecular Biology of the Cell
Vol. 20, 3251–3260, July 15, 2009

Endocytic Accessory Proteins Are Functionally Distinguished by Their Differential Effects on the Maturation of Clathrin-coated Pits

Marcel Mettlen,* Miriam Stoeber,*† Dinah Loerke, Costin N. Antonescu, Gaudenz Danuser, and Sandra L. Schmid

Department of Cell Biology, The Scripps Research Institute, La Jolla, CA 92037

Submitted March 31, 2009; Revised May 8, 2009; Accepted May 12, 2009
Monitoring Editor: Sandra Lemmon

Diverse cargo molecules (i.e., receptors and ligand/receptor complexes) are taken into the cell by clathrin-mediated endocytosis (CME) utilizing a core machinery consisting of cargo-specific adaptors, clathrin and the GTPase dynamin. Numerous endocytic accessory proteins are also required, but their differential roles and functional hierarchy during CME are not yet understood. Here, we used a combination of quantitative live-cell imaging by total internal reflection fluorescence microscopy (TIR-FM), and decomposition of the lifetime distributions of clathrin-coated pits (CCPs) to measure independent aspects of CCP dynamics, including the turnover of abortive and productive CCP species and their relative contributions. Capitalizing on the sensitivity of this assay, we have examined the effects of specific siRNA-mediated depletion of endocytic accessory proteins on CME progression. Of the 12 endocytic accessory proteins examined, we observed seven qualitatively different phenotypes upon protein depletion. From this data we derive a temporal hierarchy of protein function during early steps of CME. Our results support the idea that a subset of accessory proteins, which mediate coat assembly, membrane curvature, and cargo selection, can provide input into an endocytic restriction point/checkpoint mechanism that monitors CCP maturation.

INTRODUCTION

Clathrin-mediated endocytosis (CME) proceeds through the sequential stages of 1) clathrin nucleation at the membrane, 2) clathrin-coated pit (CCP) maturation and invagination, 3) CCP scission, and 4) vesicle uncoating (Conner and Schmid, 2003). The core components of the CME machinery, namely clathrin, the tetrameric adaptor protein AP-2, and the large GTPase dynamin, are assisted by numerous endocytic accessory proteins throughout all stages of CCP maturation (Schmid and McMahon, 2007). Although the function of the core components of the CME machinery is increasingly well understood, the exact function of most other endocytic accessory proteins remains unknown. Among these factors, some such as CALM, epsin1, and SNX9 recognize specific subclasses of cargo molecules (Howard *et al.,* 1999; Harel *et al.,* 2008; Kazazic *et al.,* 2009). Others, such as intersectin, Eps15, SNX9, and endophilin have multiple protein-interaction domains (e.g., Eps15-homolgy [EH] or Src-homology 3 [SH3] domains) and are thought to have scaffolding functions (Miliaras and Wendland, 2004; Ungewickell and Hinrichsen, 2007). Endophilin, SNX9, and epsin have lipid curvature sensing and/or generating domains (e.g., BAR or ENTH domains) and are thought to regulate CME by introducing local biochemical and physical changes into the lipid bilayer, i.e., membrane curvature (Ford *et al.,* 2002; Itoh and De Camilli, 2006). Finally, Hip1R, SNX9, and intersectin are thought to link CME to the actin cytoskeleton and actin dynamics (McPherson, 2002; Le Clainche *et al.,* 2007; Yarar *et al.,* 2007). How these diverse and partially redundant components of the endocytic machinery are integrated and function to create a robust mechanism for CCP initiation and maturation is unclear.

Biochemical assays have shown that overexpression or small interfering RNA (siRNA) knockdown of the various endocytic accessory proteins inhibit, to varying degrees, the overall rate of CME, typically assessed by internalization of transferrin (Huang *et al.,* 2004; Engqvist-Goldstein *et al.,* 2004; Soulet *et al.,* 2005). However, these quantitative differences in the requirements of the various accessory factors for the overall efficiency of CME provide little insight into how the factors might differ qualitatively in their function and whether they act at different stages during CCP maturation. Moreover, siRNA knockdown of some accessory proteins showed only moderate or no effects on CME, making conclusions regarding their function difficult and ambiguous. More sensitive in vivo assays are needed to detect milder

This article was published online ahead of print in *MBC in Press* (http://www.molbiolcell.org/cgi/doi/10.1091/mbc.E09–03–0256) on May 20, 2009.

* These authors contributed equally to this work.

Author contributions: M.S., C.A., and M.M. performed all the cell biological, biochemical, and microscopic assays; D.L. designed and wrote the lifetime analysis software; M.M., M.S., and D.L. carried out data processing; S.L.S. and G.D. provided experimental design and assistance in interpretation; M.M. prepared the figures; M.M., M.S., D.L., G.D., and S.L.S. wrote the manuscript.

† Present address: ETH, Institute for Biochemistry, Schafmattstraße, 18, 8093 Zurich, Switzerland.

Address correspondence to: Sandra L. Schmid (slschmid@scripps.edu).

Abbreviations used: CCP, clathrin-coated pit; CCV, clathrin-coated vesicle; CME, clathrin-mediated endocytosis; TIR-FM, total internal reflection fluorescence microscopy.

phenotypes due to incomplete knockdown and/or partial redundancy in protein function. Together with a higher temporal resolution to resolve early stages of CCP maturation, these assays could provide better insight into the differential roles of these endocytic accessory proteins in CME.

Several studies have used microscopy-based assays and fluorescently tagged proteins to dissect the spatiotemporal organization of single CCPs in living cells (Merrifield *et al.*, 2002; Kaksonen *et al.*, 2003; Soulet *et al.*, 2005; Rappoport *et al.*, 2008). This approach has been especially successful when combined with genetic knockout studies in yeast (Kaksonen *et al.*, 2003, 2005; Rappoport *et al.*, 2008). Because individual endocytic events in yeast occur in a relatively invariant, stereotypical manner, these analyses have enabled the clustering of endocytic accessory factors into temporally and functionally distinct subsets. In contrast, fluorescent studies on CME in mammalian cells have revealed significant dynamic heterogeneity (Gaidarov *et al.*, 1999; Merrifield *et al.*, 2002; Keyel *et al.*, 2004; Yarar *et al.*, 2008; Loerke *et al.*, 2009). We have recently developed methods that exploit this dynamic heterogeneity to gain insight into the function of various endocytic components in the CCP maturation process. By decomposition of the measured CCP lifetime distributions, we identified three kinetically distinct subpopulations: two short-lived abortive populations and a longer-lived productive population (Loerke *et al.*, 2009). Manipulation of cargo and adaptor protein concentration and analysis of dynamin mutants suggested that CCP maturation is gated by an "endocytic restriction/checkpoint", which is sensitive to cargo loading and regulated by dynamin. The finding that our manipulations differentially affected either the fraction of the three CCP subpopulations or their lifetimes indicated that these are independent parameters that can be measured to establish a functional hierarchy of CME factors. For example, perturbations that increase the lifetimes of productive CCPs and/or decrease their fractional contribution are likely to be limiting components for CCP maturation. In contrast, factors that are sensed by the endocytic restriction/checkpoint apparatus would be expected to affect the rate of turnover of abortive CCPs.

Here, we use this assay to identify the differential effects of siRNA-repressed expression levels of 10 endocytic accessory proteins: SNX9, epsin1, Hip1R, Eps15, intersectin2, CALM, endophilin, GAK, and clathrin light chain a and b (LCa and LCb, respectively). Our data provide new insight into the regulatory roles of these accessory proteins in clathrin-coated vesicle (CCV) formation.

MATERIALS AND METHODS

Cell Lines and Cell Culture

Epithelial BSC1 monkey kidney cells stably expressing rat brain clathrin LCa fused to enhanced green fluorescent protein (LCa-EGFP) or the AP-2 rat brain σ2-adaptin fused to EGFP were kindly provided by Dr. T. Kirchhausen (Harvard Medical School). Cells were grown under 5% CO_2 at 37°C in DMEM supplemented with 20 mM HEPES, 10 μg/ml streptomycin, 66 μg/ml penicillin, 10% (vol/vol) fetal calf serum (FCS, Hyclone, Logan, UT) and 0.5 mg/ml geneticin (Invitrogen, Carlsbad, CA).

siRNA and Transfection

siRNA duplexes (Dharmacon Research, Boulder, CO, and Invitrogen) were 1) chosen according to published sequences, 2) derived from a Dharmacon "ON-TARGET plus Set of 4", or 3) personally designed by using the online Stealth siRNA Designer (https://rnaidesigner.invitrogen.com/rnaiexpress/). The following sequences were used: endophilin: GCA CAU UGU CAA AGG UCA ATT (Wang *et al.*, 2003); epsin1: GAU CAA GGU UCG AGA GGC CTT (Dharmacon "Set of 4"); Eps15: UUG ACC UUU GAC AAU GUG CTT (Huang *et al.*, 2004); GAK: GCG ACA CGG UUC UGA AGA UTT (Dharmacon "Set of 4"); Hip1R: UGG CUG ACC UCU UCG AUC AUU (Dharmacon "Set of 4"); SNX9: AGA GCU ACA UCG AAU AUC ATT (Yarar *et al.*, 2007); CLCa: GCA GAA GAA GCC UUU GUA ATT (Huang *et al.*, 2004); CLCb: GGA ACC AGC GCC AGA GUG AUU (Huang *et al.*, 2004); CALM: AAG GAT AAA AGT GGA TTG CAA (Qiagen, Chatsworth, CA); and intersectin2: AAC GTA AAG CCC AGA AAG AAA (Qiagen).

The day before transfection, 8×10^4 BSC1 cells were plated in a 60-mm Petri dish. On day 1 and day 3, cells were washed with Opti-MEM (Invitrogen) and transfected using 50 nM siRNA and 12 μl HiPerFect transfection reagent (Qiagen) in a total volume of 2 ml Opti-MEM, according to the manufacturer's recommendations. After a 5-h incubation, cells were washed with culture medium and split if necessary. Cells were analyzed by Western blot or total internal reflection fluorescence microscopy (TIR-FM) 72 h after the first transfection.

SDS-PAGE and Western Blot

To detect levels of specific protein depletion after siRNA treatment, cells were lysed (50 mM Tris-base, 2 mM EGTA, 150 mM NaCl, 1% Nonidet P40, 10 mM NaF, 2 mM Na-vanadate, 0.25% deoxycholic acid, Complete protease inhibitor [Roche, Indianapolis, IN], pH 7.4) and sonicated, and remaining cell debris was spun down. Total protein concentration was determined, and equal amounts of cell lysates were separated using SDS-PAGE (10 or 12% gels), transferred to a nitrocellulose membrane (Whatman, Clifton, NJ), blocked for 1 h at room temperature in Western blot buffer (20 mM Tris-Base, 15 mM NaCl, 5 mM EDTA, and 0.5% Tween-20, pH 7.4), supplemented with 5% skim milk, and incubated with primary antibodies overnight (anti-actin, Chemicon International, Temecula, CA; endophilin2, kindly provided by Prof. P. De Camilli (Yale University School of Medicine); epsin1, Eps15, CLCs, CALM, and Snx9, from the Schmid lab; GAK, Medical & Biological Laboratories, Nagoya, Japan; Hip1R, kindly provided by Prof. D. Drubin (University of California, Berkeley); intersectin, Novus Biologicals, Littleton, CO; and dynamin3, Abcam, Cambridge, MA, [which recognizes a 100-kDa nonspecific band that serves as a loading control, referred to as Ab-Cam antigen]). The blots were revealed by HRP-labeled secondary antibodies and enhanced chemiluminescence. For a rigorous quantification, chemiluminescent blots were analyzed by an Alpha Innotech FluorChem SP image station and the values for respective silencing efficiency were obtained using ImageJ (NIH; http://rsb.info.nih.gov/ij/) image analysis software. The protein band intensity of the silenced protein was normalized to the respective loading control (actin or the Ab-Cam antigen), averaged among the different lysate dilutions and, in order to obtain the percentage of silencing, compared with the expression levels in control cells that were treated with nonrelated siRNA.

Live Cell Imaging by TIR-FM

Cells were prepared for TIR-FM as previously described (Loerke *et al.*, 2009). In brief: the day before imaging, 80,000 BSC1 cells were seeded per well in six-well plates containing a 22 × 22-mm glass coverslip. The next day, cells were washed three times with PBS, incubated with imaging medium, and mounted on coverslips. For imaging, the cells were rapidly transferred to a prewarmed microscope stage (37°C; controlled with a custom-modified stage incubator), and four to seven cells were imaged per coverslip. TIR-FM movies of BSC1 cells stably expressing LCa-EGFP or σ2-EGFP were acquired in fast (frame rate, 400 ms; exposure time, 90 ms) and slow (frame rate, 2 s; exposure time, 200 ms) acquisition mode during 10 min, using a 100× 1.45 NA objective (Nikon, Melville, NY) mounted on a Nikon TE2000U inverted microscope (Nikon, Melville, NY) and a 14-bit mode-operated Hamamatsu Orca II-ERG camera (Hamamatsu Photonics, Hamamatsu City, Japan). For every silencing condition, at least 18 movies of different cells from a minimum of three independent silencing experiments were recorded. Movies of control cells treated with nonrelevant siRNA were routinely recorded in parallel with experimental conditions. For acquisition of epifluorescence (EPI)-TIR-FM movies upon GAK depletion, pairs of EPI- and TIR-FM images (exposure times, 200 ms) were acquired sequentially for 10 min, with 2-s intervals between pairs and 30−0ms delay between EPI and TIR-FM acquisition.

Automated Image and CCP Lifetime Analysis

Fluorescent particle detection and life-time tracking of CCPs in the TIR-FM movies was accomplished using the software package described in (Jaqaman *et al.*, 2008). The lifetime analysis of CCPs was performed according to previous studies (Loerke *et al.*, 2009).

Statistical Analyses

Significant subpopulations were identified by minimization of the value of the Bayesian information criterion (BIC) as described in (Loerke *et al.*, 2009). The lifetime decomposition yields time constants [δ_1, δ_2, …, δ_n] and contributions [c_1, c_2, …, c_n] of the (generally three) CCP subpopulations and the contribution c_p of the persistent population; these parameters are calculated by fitting the lifetime histogram, pooled from multiple cells, to the appropriate number of (Weibull-shaped) distributions.

It is not completely straightforward to define a meaningful error for the parameters. The simplest approach for calculating a meaningful cell-to-cell error Δq for each of the parameters q would be to fit the lifetime histograms of each cell individually, and to then calculate Δq as the SD of the resulting distribution of parameters. However, in our case a minimum of two movies (one fast, one slow) is required to construct one complete histogram suitable

for data fitting. Furthermore, as discussed in (Loerke *et al.*, 2009) many more cells and an n >5000 are required to guarantee stable convergence of the model selection step. Therefore, we use the jackknife method for error determination (Thomson and Chave, 1991), a special case of a bootstrap assay. If q is the parameter of interest (e.g., the time constant of population 2), $\hat{q}_{all}$ is the estimate using all observations, and $\hat{q}_i$ is the estimate using all observations except i, i.e., the parameter is calculated by fitting the lifetime histogram pooled from all movies except movie i.

The jackknife variance

$$\mathrm{var}\{\hat{q}_{all}\} = \frac{N-1}{N}\sum_{i-1}^{N}\left[\hat{q}_i - q_{\hat{}}\right]^2 \quad \text{where} \quad q_{\hat{}} = \frac{1}{N}\sum_{i-1}^{N}\hat{q}_i$$

is an accurate and conservative estimate of the true variance of $\hat{q}_{all}$. Moreover, the distribution of the jackknifed parameter estimation approximates a normal distribution because of the central limit theorem. As a result, the p-value of the difference of a certain parameter between two conditions can be assayed by a *t* test approach, as follows:

The means and jackknife-estimated variances of the parameter in condition one and two are $[\bar{q}_1, \bar{q}_2]$ and $[\mathrm{var}_1, \mathrm{var}_2]$; the sample sizes (number of cells/movies) in the two conditions are $[n_1, n_2]$.

The SE for unequal sample size and unequal variance is

$$S_{12} = \sqrt{\frac{\mathrm{var}_1}{n_l} + \frac{\mathrm{var}_2}{n_2}}$$

The t-statistic is $t = (\bar{q}_1 - \bar{q}_2)/S_{12}$, and the relevant degrees of freedom are (as the most conservative estimate) $d = \min[(n_1 - 1), (n_1 - 1)]$.

Thus, the p-value for this *t*-statistic and for the specified degrees of freedom is defined as one minus the integral of the probability density function of the *t*-distribution between [−t, t].

RESULTS

Using epithelial BSC1 cells stably expressing EGFP-tagged clathrin light chain (LCa-EGFP; Ehrlich *et al.*, 2004), we recorded time-lapse movies of fluorescently labeled CCPs by TIR-FM. CCP trajectories were obtained using automated particle tracking (Jaqaman *et al.*, 2008). As described previously (Loerke *et al.*, 2009), we then applied statistical model selection to decompose the lifetime distribution of the entire tracked population into subpopulations with distinct lifetimes. When applied to the distribution of CCPs in control cells (100,823 CCP trajectories pooled from 65 different cells), the model selection identified three significant CCP subpopulations (Figure 1A), consistent with previous results (Loerke *et al.*, 2009). Accordingly, we designated the subpopulations as early abortive, late abortive, and productive CCPs. As shown in Figure 1B, productive CCPs, which lead to vesicle formation, contribute 47.8 ± 1.9% (mean ± jackknifed cell-to-cell error; Thomson and Chave, 1991) to the total number of CCPs found at the plasma membrane, with early and late abortive CCPs representing 32.0 ± 1.1 and 18.6 ± 1.5%, respectively. The remaining CCPs (1.6 ± 0.1%) were designated "persistent," because they failed to turnover for the duration of the 10-min movies (Supplementary Figure S1A). The measured time constants were 5.7 ± 0.2 and 18.5 ± 1.3 s for early and late abortive CCPs, respectively, whereas the longer-lived, productive subpopulation was characterized by a time constant of 62.4 ± 2.2 s (Figure 1C). Treatment of cells with nonrelevant siRNA had no effect on the productive subpopulation, but modest, although significant, effects on the relative contribution and lifetime of early and late abortive CCPs, respectively (Figure 1, B and C). Nonetheless, as a rigorous control, all treatments hereafter have been compared with nonrelevant siRNA-treated cells.

Compared with previous analysis of the same cell system (Loerke *et al.*, 2009), the relative contribution and the mean lifetimes of productive CCPs increased and decreased, respectively, suggesting an overall increase in the efficiency of CME in this new set of experiments. These changes are likely

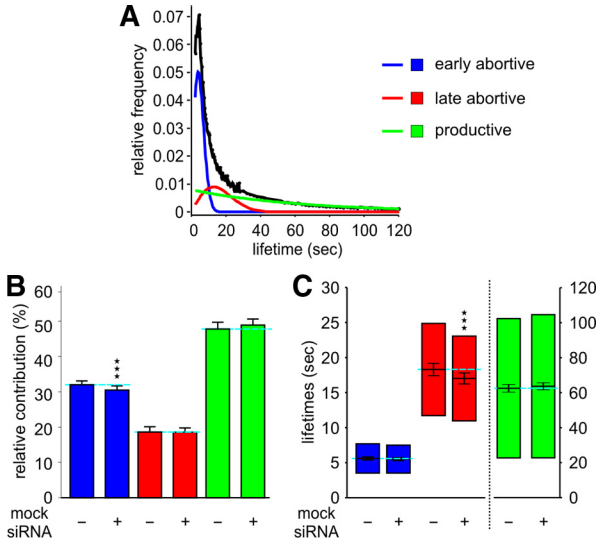

Figure 1. Decomposition of CCP lifetime distributions indicates three subpopulations of CCPs in control and nonrelevant siRNA-treated cells. (A) Lifetime distribution of CCP trajectories in control cells and identification of three subpopulations of CCPs, termed early abortive (blue); late abortive (red) and productive CCPs (green). (B) Relative contributions and (C) lifetimes of CCP subpopulations in control (same as in A) and nonrelevant siRNA-treated cells. Error bars represent cell-to-cell variation; the length of the lifetime bars in C denotes the t_{50}-spread of the distribution, i.e., the range around the characteristic lifetime that contains 50% of the data. The number of CCP trajectories (n) and cells (k) for each condition are control (n = 100,823, k = 65) and nonrelevant siRNA (n = 117,835, k = 92). *** $p < 10^{-8}$. This high level of confidence was chosen because the high content of our analysis (especially under control and nonrelevant siRNA-treated conditions), renders even small differences statistically significant.

to reflect differences in cell culture conditions and/or a clonal cell population. Thus, we were careful to perform control experiments in parallel with each perturbation condition, so that the values reported here were reproducible and consistent from experiment to experiment and from cell to cell.

Using this assay, we previously showed that siRNA depletion of two core components of the endocytic machinery, AP-2 and dynamin, had dramatically different effects on CCP dynamics. AP-2 depletion (by 50%) reduced the total number of CCPs without affecting either the proportion or the lifetimes of the three subpopulations (Loerke *et al.*, 2009). In contrast, siRNA depletion of dynamin (by ~70%) had no effect on the number of CCPs or on the proportion of abortive versus productive CCPs, but increased the lifetimes of both abortive and productive subpopulations. These differential phenotypes are consistent with the well-established role for AP-2 as a critical and limiting structural component required to initiate CCP assembly and with a role for dynamin in regulating CCP maturation. To better define the distinct functions of the less well-studied endocytic accessory factors, we examined the effects of their knockdown on the distinct aspects of CCP dynamics.

Early and Late Stages of CCP Maturation Are Affected by Depletion of SNX9, CALM, or Epsin

SNX9 is an SH3 domain– and BAR domain–containing protein that interacts with dynamin and promotes its GTPase activity (Soulet *et al.*, 2005; Lundmark and Carlsson, 2009). In

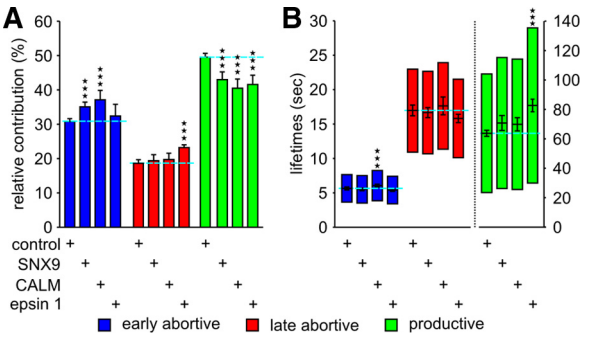

Figure 2. SNX9, CALM and epsin1 depletion strongly decrease CCP maturation efficiency. (A) Relative contributions and (B) lifetimes of CCP subpopulations in cells treated with either nonrelevant siRNA (control), SNX9 siRNA, CALM siRNA, or epsin1 siRNA, as indicated. The number of CCP trajectories (n) and cells (k) for each condition are control (n = 117,835, k = 92), SNX9 (n = 50,975, k = 25), CALM (n = 40,528, k = 26), and epsin 1 (n = 34,930, k = 18). *** $p < 10^{-8}$.

vivo studies have shown a concomitant burst of SNX9 and dynamin recruitment to CCPs during late stages of CCV formation (Soulet *et al.*, 2005). As a member of the sorting nexin family, SNX9 has also been shown to interact with different cell surface transmembrane proteins and may play a role in directing their endocytosis (Howard *et al.*, 1999). CALM is the nonneuronal homologue of AP180 (Assembly Protein 180 kDa) and functions in coat assembly and in recognition of v-SNAREs, a specialized cargo component of CCVs, through its ANTH domain (Harel *et al.*, 2008). Finally, epsin1 is an EH domain–binding partner that interacts with both Eps15 and intersectin (Chen *et al.*, 1998; Yamabhai *et al.*, 1998; Nakashima *et al.*, 1999). It is thought to induce membrane curvature by binding of PtdIns(4,5)P2 through its ENTH domain and insertion of an N-terminal amphipathic helix into the inner leaflet of the lipid bilayer (Ford *et al.*, 2002; Stahelin *et al.*, 2003). It also has a ubiquitin-binding motif involved in recruiting ubiquinated cargo molecules to CCPs (Hawryluk *et al.*, 2006; Chen and Zhuang, 2008; Kazazic *et al.*, 2009).

We used siRNA treatment to individually reduce the cellular levels of these proteins and examined the effects on CCP dynamics. For all experiments described herein, we assayed cells 72 h after a double-round siRNA treatment. Although this protocol resulted in only partial knockdown of expression levels (Supplementary Figure S2), the sensitivity of our assay nonetheless enabled us to detect reproducible and statistically significant effects (see Figures 1–4, *** $p < 10^{-8}$). Strong perturbations that potently inhibit CME were avoided because they increase the percentage of persistent CCPs and may result in indirect effects due to depletion of other limiting factors. We also confirmed that siRNA knockdown of the endocytic accessory proteins described herein did not dramatically alter overall CCP density (Supplementary Figure S1B).

Reduction of the cellular SNX9 pool by 35% significantly decreased the relative contribution of productive CCPs, with a corresponding increase in early abortive species and no effects on their lifetimes (Figure 2, A and B). We also detected a slight ($p = 1.7 \times 10^{-5}$) increase of productive lifetimes. Although this change did not fall under the here fixed threshold of significance, we expect that higher knockdown efficiency would increase this difference, as was previously shown biochemically (Soulet *et al.*, 2005). Similar effects were observed upon depletion of CALM by 60% relative to initial cellular expression levels, but the strongly increased early abortive population displayed a significantly slower turnover rate (Figure 2, A and B). The effect of depletion of these proteins on early abortive CCPs provides strong evidence that these short-lived structures are indeed related to CME and not internal clathrin-coated structures transiently appearing in the evanescent field. Partial depletion of epsin1 by 40% also decreased the efficiency of CCP maturation with corresponding increases in the fraction of predominantly late abortive CCPs (Figure 2A). Like SNX9 and CALM, depletion of epsin1 also increased the lifetimes of productive CCPs, albeit to a greater degree (Figure 2B), suggesting that its expression levels are more critical in CCV formation. Consistent with this, depletion of epsin1 also increased the relative contribution of persistent CCPs by 47% to 2.8 ± 0.3%, whereas the effect of SNX9 or CALM depletion on these CCPs was not significant (Supplementary Figure S1A). These data suggest that each of these factors is, albeit to varying extents, limiting for CCP maturation.

Depletion of Hip1R, Eps15, or Intersectin2 Slows CCP Maturation

Hip1R functions at the interface between the actin cytoskeleton and the endocytic machinery through direct and simultaneous binding to both clathrin and F-actin (Engqvist-Goldstein *et al.*, 2004). As previously reported, we observed that reduced levels of Hip1R cause unusual actin structures that stably anchor CCPs at the plasma membrane (data not shown; Engqvist-Goldstein *et al.*, 2004). As a scaffolding protein, Eps15 brings together different components of the clathrin-dependent endocytic machinery. Its N-terminal region contains three copies of the protein–protein interaction module, the EH domain. Both the depletion of Eps15 (Carbone *et al.*, 1997; Huang *et al.*, 2004) and the overexpression of truncated forms (Benmerah *et al.*, 1999) impair the uptake of Tfn receptors. Intersectins are large molecules believed to function as scaffolding proteins at sites of CCP formation. In addition to three conserved EH domains and five SH3 domains (Guipponi *et al.*, 1998; Yamabhai *et al.*, 1998) that mediate interactions with, among others, dynamin (Yamabhai *et al.*, 1998; Okamoto *et al.*, 1999; Sengar *et al.*, 1999), intersectins interact with the actin regulatory proteins N-WASP and Cdc42 and have been shown to regulate actin assembly (Hussain *et al.*, 2001; McGavin *et al.*, 2001).

In contrast to the results reported above, depletion of Hip1R, Eps15, and intersectin2 by 55, 75, and 45%, respectively (Supplementary Figure S2), had no significant effect on the proportion of productive CCPs, but all three treatments significantly increased their lifetimes (Figure 3, A and B). In line with previous observations, we also observed an increase in the relative contribution of persistent CCPs from 1.9 ± 0.2% in control siRNA-treated cells to 2.7 ± 0.4% in Hip1R-depleted cells, and to 3.2 ± 0.4% after intersectin2 siRNA-treatment, whereas Eps15 depletion did not affect this population (Supplementary Figure S1A). We did not detect any effect of siRNA knockdown of intersectin1 (data not shown). Together, these phenotypes suggest that the functions of these proteins are restricted to, and are rate-limiting, for late events in CCV formation, but that they may not be limiting for early events in CCP maturation.

Endophilin Specifically Functions during Early Events, Whereas GAK Functions at Both Early and Late Stages in CCV Formation

The dynamin-binding partner endophilin has been suggested to have an early role in membrane curvature generation, because microinjection of endophilin antibodies in axon nerve terminals resulted in the striking accumulation

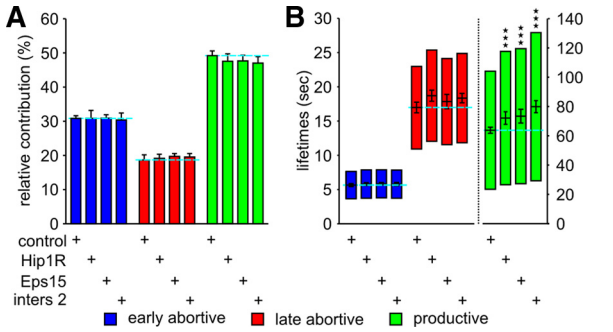

Figure 3. Hip1R, Eps15, and intersectin2 depletion strongly decrease productive CCP maturation speed without affecting abortive CCPs. (A) Relative contributions and (B) lifetimes of CCP subpopulations in cells treated with the indicated siRNA. The number of CCP trajectories (n) and cells (k) for each condition are control (n = 117,835, k = 92), Hip1R (n = 37,958, k = 23), Eps15 (n = 36,278, k = 21), and intersectin2 (n = 35,499, k = 28). *** $p < 10^{-8}$.

of shallow CCPs (Ringstad *et al.*, 1999). This effect might be mediated by its N-terminal BAR domain (Gallop *et al.*, 2006), known to sense and generate membrane curvature. Endophilin depletion by 50% had no effect on the relative proportions of abortive and productive events and no significant effect on the lifetime of productive CCPs. However, we observed a dramatic increase in the rate of turnover of late abortive CCPs (Figure 4, A and B). In contrast to the findings for intersectin2, Hip1R, and Eps15, these results point to an early and critical function for endophilin that is sensed by the restriction/checkpoint apparatus and indicate that endophilin function is not rate-limiting during later stages of CCV formation.

The multifunctional cyclin G–associated kinase, GAK, is the nonneuronal homologue of the cochaperone auxilin, which recruits Hsc70 to assembled clathrin, thereby disrupting clathrin–clathrin interactions and inducing clathrin uncoating (Ungewickell *et al.*, 1995; Jiang *et al.*, 2000; Umeda *et al.*, 2000). In addition, GAK has been shown to be involved in early steps of CME by recruiting both clathrin and clathrin adaptors to CCPs and mediating clathrin exchange during CCP maturation (Lee *et al.*, 2005). Finally, GAK encodes a kinase domain (Zhang *et al.*, 2005) that is homologous to the AAK1 kinase, which phosphorylates the μ2 subunit of

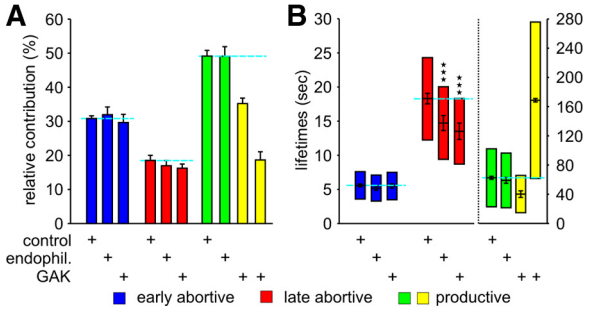

Figure 4. Endophilin and GAK increase turnover of late abortive CCPs. (A) Relative contributions and (B) lifetimes of CCP subpopulations in cells treated with the indicated siRNA. In contrast to all other conditions, the BIC-based model selection identified four CCP subpopulations upon GAK depletion. The number of CCP trajectories (n) and cells (k) for each condition are control (n = 117,835, k = 92), endophilin (n = 49,014, k = 22), and GAK (n = 54,141, k = 31). *** $p < 10^{-8}$.

AP-2 (Conner and Schmid, 2002). Knockdown of GAK by 80% resulted in a novel set of phenotypes. Similar to endophilin, GAK depletion strongly increased the rate of turnover of late abortive CCPs, without affecting their relative contribution, suggesting an early function sensed by the restriction/checkpoint apparatus. The most dramatic phenotype, however, was that the BIC-based model selection detected a fourth, long-lived CCP subpopulation. As for productive CCPs in control cells, the new fourth population could be described by an exponentially decaying distribution with a mean time constant of 171.0 ± 2.5 s (Figure 4B). Of note, the sum of the relative contributions of the two long-lived subpopulations (P3 = 35.8 ± 12.1% and P4 = 16.2 ± 1.1%) perfectly matched the relative contribution of the single productive subpopulation in control cells (i.e., 53.4 ± 2.6%; Figure 4B). In addition, because internalization can be verified by sequential disappearance from the TIR-FM and the EPI-FM field (Merrifield *et al.*, 2002; Yarar *et al.*, 2005), we applied automated tracking to nearly simultaneously acquired EPI/TIR-FM movies (see *Materials and Methods*) and analyzed 359 CCPs with lifetimes of 140–180 s. Comparison of EPI and TIRF signal intensities clearly showed a ~20 s delay in the disappearance of clathrin-coated structures first from the TIRF field and then from the EPI field (data not shown), confirming that these very long-lived CCPs internalized as regular CCVs. We therefore assume that after GAK silencing, the two long-lived CCP populations resulted from a split of the productive CCP population into a fast (mean lifetime of 40.1 ± 4.5 s) and a slow productive CCPs (mean lifetime of 171.0 ± 2.5 s; Figure 4B). Together these data suggest that GAK plays both early and late, rate-limiting roles in governing CCP maturation.

Clathrin LCa or LCb Depletion Causes Distinct Phenotypes

The clathrin triskelion is composed of three clathrin heavy chains (CHCs), each bound to one of two clathrin light chain (CLC) isoforms, designated CLCa and CLCb. Although the precise function of the two CLC isoforms is unknown, they might play a regulatory role in clathrin polymerization (Wilbur *et al.*, 2008). Biochemical assays for transferrin internalization have detected only mild, if any, effects upon siRNA depletion of either or both CLCs (Huang *et al.*, 2004). To examine the effect of CLC depletion using our more sensitive TIRF-based assay, we carried out siRNA-mediated knockdown of CLCa or CLCb in BSC1 cells stably expressing the AP-2 subunit σ2, tagged with EGFP (σ2-EGFP). As a major component of CCPs, AP-2 colocalizes with clathrin at the forming pit, and CCP trajectories can be tracked and analyzed in the same manner as LCa-EGFP–labeled CCPs (Loerke *et al.*, 2009). In agreement with previous results in control cells, our BIC-based model selection identified three kinetically distinct subpopulations of σ2-EGFP–labeled CCPs in cells treated with nonrelevant siRNA. Also as reported earlier (Loerke *et al.*, 2009), CCP lifetimes were generally shorter when σ2-EGFP was tracked (cf. Figures 1C and 5B). Depletion of the CLCa isoform by ~50% resulted in a significant ($p < 10^{-6}$; threshold was set lower compared with previous figures because of the smaller sample size) increase in the relative contribution of productive CCPs without significantly affecting their lifetimes (Figure 5, A and B). In contrast, depletion of the CLCb isoform decreased the lifetimes of productive CCPs, without altering their relative contributions. Both of these effects would slightly increase the efficiency of CME, suggesting that the CLCs might function as negative regulators of CME. Interestingly, the two CLC isoforms also had very different effects on the

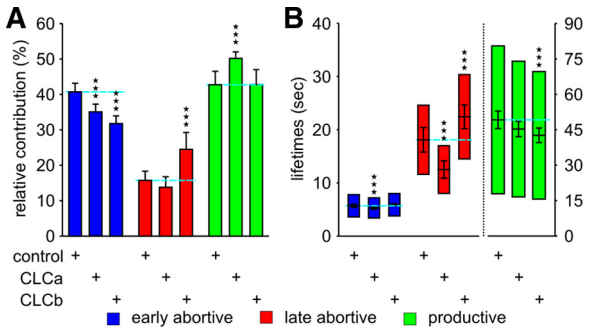

Figure 5. CLCa and CLCb depletion in BSC1-σ2-EGFP cells differentially affect turnover of late abortive CCPs. (A) Relative contributions and (B) lifetimes of CCP subpopulations in cells treated with the indicated siRNA. The number of CCP trajectories (n) and cells (k) for each condition are control (n = 43,477, k = 33), CLCa (n = 32,782, k = 23), andCLCb (n = 20,638, k = 21). *** $p < 10^{-6}$.

abortive CCP subpopulations. Depletion of CLCa resulted in a significant decrease in the mean lifetime of early and late abortive CCPs, whereas CLCb depletion had the opposite effect and increased the lifetimes of late abortive species. Depletion of CLCb also increased the proportion of late abortive species at the expense of early abortive CCPs, which is consistent with the delayed rate of turnover of abortive species. Thus, both light chains appear to provide input into the endocytosis restriction/checkpoint apparatus, but evoke differential responses: CLCa depletion activates turnover, whereas CLCb depletion delays turnover of abortive species.

DISCUSSION

Endocytic Accessory Factors Differentially Affect CCP Dynamics

The present study begins to address the differential roles of endocytic accessory factors during CCV formation. By TIRF time-lapse microscopy, particle tracking, and statistical model selection we have analyzed how lifetimes and relative contributions of three distinct CCP subpopulations are altered upon siRNA-mediated depletion of specific endocytic accessory proteins. The high sensitivity of this assay was a prerequisite for the present study, because only mild perturbations (i.e., partial knockdown, see Supplementary Figure S2) were applied to probe the function of proteins. This minimized the risk of uncontrolled nonlinear responses that may be induced by stronger perturbation of a tightly integrated, multifactorial assembly cascade. In contrast to previous siRNA studies, where 90–95% silencing efficiencies of accessory proteins were needed to elicit significant biochemical effects on CME (e.g., Huang *et al.*, 2004), the milder protein knockdown (by 35–80%) conditions used in the present study were sufficient to gain insights into the functional differences of several molecular players involved in CME. The mutual independence of lifetimes and contributions of CCP subpopulations and their differential response to siRNA-mediated depletion of select components allowed us to group endocytic accessory proteins into phenotypically distinct classes (Figure 6). Strikingly, of 12 proteins studied thus far (10 from this study and two from a previous study; Loerke *et al.*, 2009), we identified seven qualitatively distinct phenotypes that suggest their differential involvement in the four aspects of CCV formation. On the basis of these effects, we propose a temporal hierarchy for endocytic accessory protein function (Figure 6). It is important to note that proteins grouped in the same class do not necessarily share common functions and/or directly interact with each other.

Our previous work had shown that a 50% siRNA-mediated knockdown of AP-2 changed neither the rate of CCV formation nor the relative contribution of CCP subpopulations (Loerke *et al.*, 2009). However the total number of CCPs at the cell membrane was proportionally reduced upon depletion of AP-2, indicating that AP-2 complexes are crucial initiators of CCP assembly and likely function in a highly cooperative manner as essential structural components for determining CCP maturation (Hinrichsen *et al.*, 2006). On

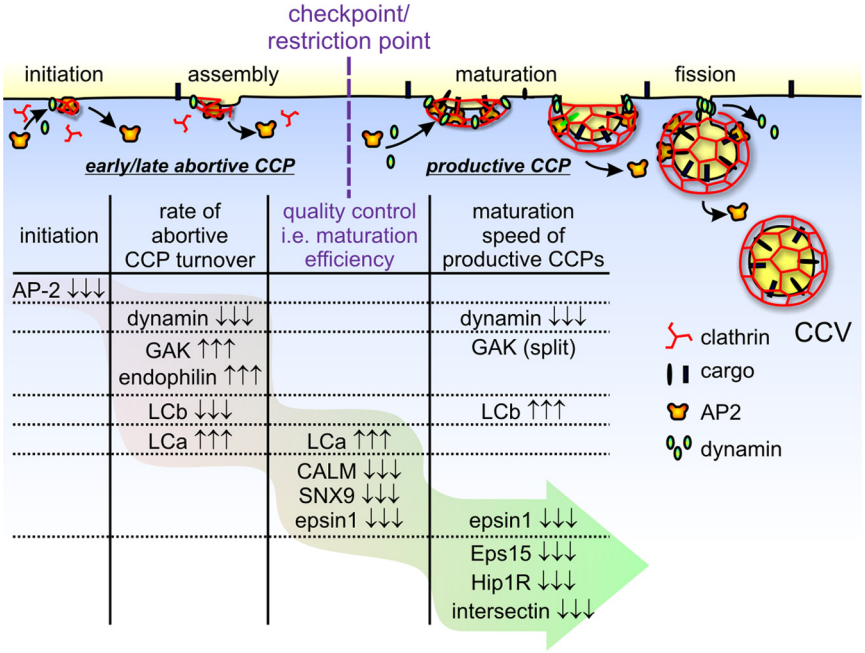

Figure 6. Accessory proteins can be grouped in distinct phenotypic classes, suggesting a temporal hierarchy of functions. We propose that CCVs are formed from productive CCPs through a maturation process gated by an endocytosis restriction point/checkpoint. CCPs that do not progress beyond this checkpoint abort. Proteins are listed and grouped according to their depletion effects on pit density (column 1); turnover rate of early and late abortive species (column 2); maturation efficiency, i.e., proportion of productive CCPs (column 3); and maturation speed of productive CCPs (column 4), which provide insight into their respective functions and temporal hierarchy of activities. Three arrows indicate a strong, significant effect. For further details, see text.

the other hand, depletion of dynamin increased the lifetime of abortive and productive CCP subpopulations, without changing their relative contributions, indicating that dynamin acts as a regulator during CCP maturation. Dynamin also functions to catalyze membrane fission (Pucadyil and Schmid, 2008); however, this step is not rate-limiting for CCV formation. No other proteins exhibited the same effects as either dynamin or AP-2, confirming the unique and critical functions of these two core components of the endocytic machinery in CME.

Depletion of Most Endocytic Accessory Proteins Decreases the Efficiency of CME

Under all conditions, with the exception of GAK depletion, the observed CCP lifetime distributions could be best fitted by a model that invokes three kinetically distinct CCP subpopulations. Knockdown of six of 12 accessory proteins (i.e., SNX9, epsin1, intersectin2, CALM, Eps15, and Hip1R; summarized in Figure 6) caused either a decrease in the relative contribution of productive CCPs and/or an increase in their lifetimes, confirming that these proteins are critical components of the machinery for CCP maturation. To varying degrees, the activities of these proteins are also rate limiting for CCV formation. This interpretation is consistent with previous biochemical studies that measured a lower overall rate of Tfn internalization after their siRNA-mediated knockdown (Huang *et al.,* 2004; Engqvist-Goldstein *et al.,* 2004; Soulet *et al.,* 2005). Those proteins whose depletion leads to a reduction in the proportion of productive CCPs (e.g., SNX9, CALM, and epsin) may play earlier roles in CCP maturation. A critical threshold of these proteins, or their respective activities, may be needed to pass the restriction/checkpoint; hence, their relative absence leads to an increase in abortive events. By contrast, those proteins whose depletion affects only the rate of maturation (e.g., Eps15, Hip1R, and intersectin2) are likely to play later roles in CCV formation and/or could mediate functions not sensed by the restriction/checkpoint apparatus.

We and others (Keyel *et al.,* 2004) have observed so-called "visitors" by which we mean intracellular CCSs that move transiently through the narrow evanescent field. These fast moving, transiently imaged structures are excluded from our analyses because we eliminate CCSs that are not detected for at least five successive frames. In contrast, we have previously argued (Loerke *et al.,* 2009) that the short lived early abortive CCPs correspond to bona fide endocytic intermediates because they are labeled by both LCa-EGFP and σ2-EGFP, and their numbers are proportionally reduced by AP-2 knockdown. The present study provides further support that these abortive events are related to CCV formation, as their numbers are significantly increased by knockdown of SNX9 and CALM. These data suggest that although these proteins are not proportionally limiting for CCP nucleation—that is, unlike AP-2, the total density of CCPs does not decrease in proportion to their depletion (see Supplementary Figure S1B)—each may play a structural role in stabilizing early CCP intermediates and thus reducing their turnover. This is consistent with the known clathrin assembly activities of CALM and might be reflective of clathrin/AP-2 binding and scaffolding functions of SNX9.

A Subset of Accessory Proteins Affects the Turnover of Abortive CCPs

Depletion of a discrete and limited subset of proteins, namely GAK, CLCa, and endophilin, dramatically increased the rate of turnover of abortive structures. We suggest that the presence and/or activity of these endocytic accessory proteins signals more directly to the restriction/checkpoint apparatus such that their relative absence (upon knockdown) triggers more rapid turnover of incomplete CCP intermediates. These proteins, either through direct interaction with the assembling clathrin coat (GAK and CLCa) or through direct interactions with the underlying membrane (endophilin is a BAR domain–containing protein) may be able to sense critical early stages in CCP maturation that generate curvature and feed this information into the checkpoint. Because clathrin can spontaneously assemble into large, endocytically compromised flat lattices (Miller *et al.,* 1991; Chetrit *et al.,* 2009), it is attractive to speculate that the absence of curvature in the developing CCP might necessitate rapid turnover of an aberrant intermediate. Further studies are required to test this hypothesis.

GAK Silencing Causes a Split of the Productive CCP Population

The effects of ~80% knockdown of GAK were unique in that the measured lifetime distribution of CCPs could be significantly better fitted by BIC-based model selection with four kinetically distinct subpopulations. Although we do not know with certainty the functional significance of these longer-lived subpopulations, we have strong evidence that they both represent ultimately productive endocytic events. This is because 1) EPI/TIRF movies show a delay between signal disappearance first in the TIRF-, then in the EPI channel, 2) biochemical studies showed only a relatively minor defect in Tfn uptake at this level of GAK knockdown (data not shown), and 3) the contributions of the two long-lived populations in GAK-depleted cells equaled the contribution of productive CCPs in control cells. The first subpopulation of these longer-lived CCPs (comprising ~66% of productive CCPs) had a shorter mean lifetime than the single productive subpopulation in control cells. We do not think this is biologically relevant, but rather it reflects the parsing of longer-lived species into the fourth subpopulation, thereby reducing the apparent mean lifetime of the remaining subpopulation. It should also be noted that although BIC-based model selection can robustly identify the need for two productive populations for a fit of the lifetime distribution, determining their lifetimes is less precise because the fit now involves a double-exponential decay with relatively similar time scales, numerically a notoriously unstable process. The emergence of two productive CCP subpopulations after GAK depletion could be explained by two mutually nonexclusive hypotheses. First, the split of productive CCPs into two subpopulations could indicate that GAK acts cooperatively and processively to fulfilling its function on individual CCPs before being freed to move to other maturing CCPs. Thus CCPs with some initial GAK associated will tend to recruit more GAK from the reduced pool, whereas CCPs with no GAK will have to wait even longer. Thus, the very-long lived CCPs may represent the subpopulation most depleted of GAK. This interpretation is consistent with TIRF-based analyses of the dynamics of GAK/auxilin association with CCPs in which these proteins were shown to be recruited with burst kinetics at very late stages during CCP invagination (Massol *et al.,* 2006; Lee *et al.,* 2006). Alternatively, the broad lifetime distribution of the productive CCP population under control conditions may reflect functionally and/or compositionally distinct subpopulations of CCPs. In this scenario, it may be that a preexisting subclass of productive CCPs is differentially sensitive to GAK depletion. Further studies will be needed to resolve these possibilities and/or to identify other mechanisms accounting for these observations.

Depletion of GAK also significantly increased the rate of turnover of abortive CCP intermediates. This observation is consistent with its role in mediating assembly of multiple constituents of CCPs and its function in clathrin exchange during early stages of maturation (Lee *et al.*, 2005, 2006). This early function for GAK is also consistent with reports that fluorescently labeled GAK transiently associates with CCPs during early stages of maturation (Massol *et al.*, 2006). In addition, GAK interacts directly with dynamin in a nucleotide-dependent manner, and this interaction has been proposed to function at early stages of CCV formation (Newmyer *et al.*, 2003). Thus, GAK is poised to feed information into dynamin and thus to affect the endocytosis restriction/checkpoint decision.

CLCa and CLCb Function Differentially as Regulators of CME

The two light-chain isomers, CLCa and CLCb, share only 60% sequence identity, but are highly conserved between species, retaining 95–98% isoform-specific sequence identity. Although CLCs are an integral part of the basic subunit of a clathrin coat, the triskelion, their precise role is still unknown. It has been suggested that they act as negative regulators of clathrin (Brodsky *et al.*, 2001), and this is consistent with our finding that knockdown of CLCa increases the proportion of productive CCPs, whereas CLCb depletion decreases their mean lifetime. Previous biochemical studies were unable to detect a clear phenotype for either single or double siRNA knockdown of CLCs (Huang *et al.*, 2004). However, there was an increase in the rate of Tfn uptake after CLCb depletion that was not commented on by the authors, but is nonetheless consistent with our findings.

Differential effects of depletion of the CLC isoforms have thus far proven difficult to detect using biochemical assays. However, we find that knockdown of CLCa or CLCb resulted in opposite effects on the rate of turnover of abortive CCPs. The relative absence of CLCa triggers rapid turnover of abortive CCPs, whereas the relative absence of CLCb delays decision making and prolongs the lifetime of abortive species. These data suggest that both CLC isoforms can signal to the endocytosis restriction/checkpoint to either negatively or positively regulate the timing of the checkpoint decision. Further work is needed to shed light on the precise function of these two CLC isoforms.

Further Evidence for the Existence of an Endocytosis Restriction/Checkpoint

Previous studies established that the rate of turnover of abortive CCPs is dependent on the basal GTP binding and hydrolysis activities of dynamin (Loerke *et al.*, 2009). On the basis of these findings, we proposed that dynamin functions as a fidelity monitor of CCP maturation to mediate endocytosis restriction point/checkpoint decisions that gate progression to functional CCPs. As originally defined from cell cycle studies, the term "restriction point" suggests that the process will not proceed until all required steps are completed (e.g., DNA synthesis before "Start"). By comparison, the term "checkpoint" suggests that defects in the decision-making machinery would result in progression beyond the checkpoint even if essential processes are not completed (e.g., the "spindle checkpoint"), resulting in the formation of aberrant products (e.g., chromosome instability). As we do not know whether defective CCVs can be formed as a consequence of a defective checkpoint apparatus, we here use the two terms interchangeably. We further proposed (Loerke *et al.*, 2009) that dynamin—as an integral part of the checkpoint apparatus—receives input from a subset of accessory factors that sense and/or mediate coat assembly, membrane curvature, and cargo selection to determine the suitability of CCP intermediates for progression beyond the restriction/checkpoint. Of the 10 accessory proteins analyzed here, we identified seven proteins whose depletion affected either the relative contributions and/or lifetimes of abortive structures. Proteins (e.g., CALM, SNX9, and epsin1) whose depletion affects only the relative contributions of abortive versus productive events are likely to mediate different aspects of early CCP maturation that can be sensed by the checkpoint apparatus. By comparison, proteins whose knockdown affects the lifetimes of abortive species (e.g., CLCa, CLCb, GAK, and endophilin) are more likely to directly sense critical aspects of CCP maturation and to trigger CCP turnover through the checkpoint apparatus.

Our data suggests that curvature, coat assembly, and cargo may be important determining factors in CCP maturation. Of four accessory factors whose depletion strongly affected the lifetimes of abortive CCPs, three (CLCa, CLCb, and GAK) are positioned to sense clathrin assembly. The fourth (endophilin) encodes a curvature-sensing domain. Two of these proteins (GAK and endophilin) directly interact with dynamin, providing a potential mechanism for input into the checkpoint decision. CALM, SNX9, and epsin1 also encode curvature-sensing and/or curvature-generating domains. Knockdown of these proteins did not alter the rate of turnover, but increased the proportion of abortive CCPs; thus these proteins likely mediate early stages of CCP maturation that are sensed by the restriction/checkpoint apparatus. Interestingly, depletion of CALM, which functions in both coat assembly (Meyerholz *et al.*, 2005) and in recruitment of the v-SNARE, a cargo molecule that must be included in CCVs to direct fusion with their intracellular targets, also affected the turnover of early abortive CCPs. Thus, we suggest that this subset of seven proteins may provide functionally relevant input, either directly or indirectly, into the restriction/checkpoint signaling apparatus. Further biochemical studies as well as detailed image analyses of the effects of point mutations in these proteins will be needed to establish their putative roles as sensors and modulators of dynamin's enzymatic activities in order to determine how they might function as components of an endocytosis checkpoint.

ACKNOWLEDGMENTS

We thank members of the Schmid and Danuser labs for helpful discussions. This research was supported by National Institutes of Health R01 Grants GM73165 to G.D. and S.L.S.; Grants GM42455 and MH61345 to S.L.S.; and by a fellowship of the American Heart Association to M.M. M.S. was a visiting graduate student at the Scripps Research Institute in 2008 from the Ecole Supérieure de Biotechnologie de Strasbourg (ESBS) and supported by a fellowship of the German Academic Exchange Service (DAAD). This is TSRI Manuscript 20089.

REFERENCES

Benmerah, A., Bayrou, M., Cerf-Bensussan, N., and utry-Varsat, A. (1999). Inhibition of clathrin-coated pit assembly by an Eps15 mutant. J. Cell Sci. *112*(Pt 9), 1303–1311.

Brodsky, F. M., Chen, C. Y., Knuehl, C., Towler, M. C., and Wakeham, D. E. (2001). Biological basket weaving: formation and function of clathrin-coated vesicles. Annu. Rev. Cell Dev. Biol. *17*, 517–568.

Carbone, R., Fre, S., Iannolo, G., Belleudi, F., Mancini, P., Pelicci, P. G., Torrisi, M. R., and Di Fiore, P. P. (1997). eps15 and eps15R are essential components of the endocytic pathway. Cancer Res. *57*, 5498–5504.

Chen, C., and Zhuang, X. (2008). Epsin 1 is a cargo-specific adaptor for the clathrin-mediated endocytosis of the influenza virus. Proc. Natl. Acad. Sci. USA *105*, 11790–11795.

Chen, H., Fre, S., Slepnev, V. I., Capua, M. R., Takei, K., Butler, M. H., Di Fiore, P. P., and De Camilli, P. (1998). Epsin is an EH-domain-binding protein implicated in clathrin-mediated endocytosis. Nature *394*, 793–797.

Chetrit, D., Ziv, N., and Ehrlich, M. (2009). Dab2 regulates clathrin assembly and cell spreading. Biochem. J. *418*, 701–715.

Conner, S. D., and Schmid, S. L. (2002). Identification of an adaptor-associated kinase, AAK1, as a regulator of clathrin-mediated endocytosis. J. Cell Biol. *156*, 921–929.

Conner, S. D., and Schmid, S. L. (2003). Regulated portals of entry into the cell. Nature *422*, 37–44.

Ehrlich, M., Boll, W., Van Oijen, A., Hariharan, R., Chandran, K., Nibert, M. L., and Kirchhausen, T. (2004). Endocytosis by random initiation and stabilization of clathrin-coated pits. Cell *118*, 591–605.

Engqvist-Goldstein, A. E., Zhang, C. X., Carreno, S., Barroso, C., Heuser, J. E., and Drubin, D. G. (2004). RNAi-mediated Hip1R silencing results in stable association between the endocytic machinery and the actin assembly machinery. Mol. Biol. Cell *15*, 1666–1679.

Ford, M. G., Mills, I. G., Peter, B. J., Vallis, Y., Praefcke, G. J., Evans, P. R., and McMahon, H. T. (2002). Curvature of clathrin-coated pits driven by epsin. Nature *419*, 361–366.

Gaidarov, I., Santini, F., Warren, R. A., and Keen, J. H. (1999). Spatial control of coated-pit dynamics in living cells. Nat. Cell Biol. *1*, 1–7.

Gallop, J. L., Jao, C. C., Kent, H. M., Butler, P. J., Evans, P. R., Langen, R., and McMahon, H. T. (2006). Mechanism of endophilin N-BAR domain-mediated membrane curvature. EMBO J. *25*, 2898–2910.

Guipponi, M., Scott, H. S., Chen, H., Schebesta, A., Rossier, C., and Antonarakis, S. E. (1998). Two isoforms of a human intersectin (ITSN) protein are produced by brain-specific alternative splicing in a stop codon. Genomics *53*, 369–376.

Harel, A., Wu, F., Mattson, M. P., Morris, C. M., and Yao, P. J. (2008). Evidence for CALM in directing VAMP2 trafficking. Traffic *9*, 417–429.

Hawryluk, M. J., Keyel, P. A., Mishra, S. K., Watkins, S. C., Heuser, J. E., and Traub, L. M. (2006). Epsin 1 is a polyubiquitin-selective clathrin-associated sorting protein. Traffic. *7*, 262–281.

Hinrichsen, L., Meyerholz, A., Groos, S., and Ungewickell, E. J. (2006). Bending a membrane: how clathrin affects budding. Proc. Natl. Acad. Sci. USA *103*, 8715–8720.

Howard, L., Nelson, K. K., Maciewicz, R. A., and Blobel, C. P. (1999). Interaction of the metalloprotease disintegrins MDC9 and MDC15 with two SH3 domain-containing proteins, endophilin I and SH3PX1. J. Biol. Chem. *274*, 31693–31699.

Huang, F., Khvorova, A., Marshall, W., and Sorkin, A. (2004). Analysis of clathrin-mediated endocytosis of epidermal growth factor receptor by RNA interference. J. Biol. Chem. *279*, 16657–16661.

Hussain, N. K., *et al.* (2001). Endocytic protein intersectin-l regulates actin assembly via Cdc42 and N-WASP. Nat. Cell Biol. *3*, 927–932.

Itoh, T. and De Camilli, P. (2006). BAR, F-BAR (EFC) and ENTH/ANTH domains in the regulation of membrane-cytosol interfaces and membrane curvature. Biochim. Biophys. Acta *1761*, 897–912.

Jaqaman, K., Loerke, D., Mettlen, M., Kuwata, H., Grinstein, S., Schmid, S. L., and Danuser, G. (2008). Robust single-particle tracking in live-cell time-lapse sequences. Nat. Methods *5*, 695–702.

Jiang, R., Gao, B., Prasad, K., Greene, L. E., and Eisenberg, E. (2000). Hsc70 chaperones clathrin and primes it to interact with vesicle membranes. J. Biol. Chem. *275*, 8439–8447.

Kaksonen, M., Sun, Y., and Drubin, D. G. (2003). A pathway for association of receptors, adaptors, and actin during endocytic internalization. Cell *115*, 475–487.

Kaksonen, M., Toret, C. P., and Drubin, D. G. (2005). A modular design for the clathrin- and actin-mediated endocytosis machinery. Cell *123*, 305–320.

Kazazic, M., Bertelsen, V., Pedersen, K. W., Vuong, T. T., Grandal, M. V., Rodland, M. S., Traub, L. M., Stang, E., and Madshus, I. H. (2009). Epsin 1 is involved in recruitment of ubiquitinated EGF receptors into clathrin-coated pits. Traffic *10*, 235–245.

Keyel, P. A., Watkins, S. C., and Traub, L. M. (2004). Endocytic adaptor molecules reveal an endosomal population of clathrin by total internal reflection fluorescence microscopy. J. Biol. Chem. *279*, 13190–13204.

Le Clainche, C., Pauly, B. S., Zhang, C. X., Engqvist-Goldstein, A. E., Cunningham, K., and Drubin, D. G. (2007). A Hip1R-cortactin complex negatively regulates actin assembly associated with endocytosis. EMBO J. *26*, 1199–1210.

Lee, D. W., Wu, X., Eisenberg, E., and Greene, L. E. (2006). Recruitment dynamics of GAK and auxilin to clathrin-coated pits during endocytosis. J. Cell Sci. *119*, 3502–3512.

Lee, D. W., Zhao, X., Zhang, F., Eisenberg, E., and Greene, L. E. (2005). Depletion of GAK/auxilin 2 inhibits receptor-mediated endocytosis and recruitment of both clathrin and clathrin adaptors. J. Cell Sci. *118*, 4311–4321.

Loerke, D., Mettlen, M., Yarar, D., Jaqaman, K., Jaqaman, H., Danuser, G., and Schmid, S. L. (2009). Cargo and dynamin regulate clathrin-coated pit maturation. PLoS. Biol. *7*, e57

Lundmark, R. and Carlsson, S. R. (2009). SNX9—a prelude to vesicle release. J. Cell Sci. *122*, 5–11.

Massol, R. H., Boll, W., Griffin, A. M., and Kirchhausen, T. (2006). A burst of auxilin recruitment determines the onset of clathrin-coated vesicle uncoating. Proc. Natl. Acad. Sci. USA *103*, 10265–10270.

McGavin, M. K., Badour, K., Hardy, L. A., Kubiseski, T. J., Zhang, J., and Siminovitch, K. A. (2001). The intersectin 2 adaptor links Wiskott Aldrich Syndrome protein (WASp)-mediated actin polymerization to T cell antigen receptor endocytosis. J. Exp. Med. *194*, 1777–1787.

McPherson, P. S. (2002). The endocytic machinery at an interface with the actin cytoskeleton: a dynamic, hip intersection. Trends Cell Biol. *12*, 312–315.

Merrifield, C. J., Feldman, M. E., Wan, L., and Almers, W. (2002). Imaging actin and dynamin recruitment during invagination of single clathrin-coated pits. Nat. Cell Biol. *4*, 691–698.

Meyerholz, A., Hinrichsen, L., Groos, S., Esk, P. C., Brandes, G., and Ungewickell, E. J. (2005). Effect of clathrin assembly lymphoid myeloid leukemia protein depletion on clathrin coat formation. Traffic *6*, 1225–1234.

Miliaras, N. B. and Wendland, B. (2004). EH proteins: multivalent regulators of endocytosis (and other pathways). Cell Biochem. Biophys. *41*, 295–318.

Miller, K., Shipman, M., Trowbridge, I. S., and Hopkins, C. R. (1991). Transferrin receptors promote the formation of clathrin lattices. Cell *65*, 621–632.

Nakashima, S., Morinaka, K., Koyama, S., Ikeda, M., Kishida, M., Okawa, K., Iwamatsu, A., Kishida, S., and Kikuchi, A. (1999). Small G protein Ral and its downstream molecules regulate endocytosis of EGF and insulin receptors. EMBO J. *18*, 3629–3642.

Newmyer, S. L., Christensen, A., and Sever, S. (2003). Auxilin-dynamin interactions link the uncoating ATPase chaperone machinery with vesicle formation. Dev. Cell *4*, 929–940.

Okamoto, M., Schoch, S., and Sudhof, T. C. (1999). EHSH1/intersectin, a protein that contains EH and SH3 domains and binds to dynamin and SNAP-25. A protein connection between exocytosis and endocytosis? J. Biol. Chem. *274*, 18446–18454.

Pucadyil, T. J. and Schmid, S. L. (2008). Real-time visualization of dynamin-catalyzed membrane fission and vesicle release. Cell *135*, 1263–1275.

Rappoport, J. Z., Heyman, K. P., Kemal, S., and Simon, S. M. (2008). Dynamics of dynamin during clathrin mediated endocytosis in PC12 cells. PLoS. ONE *3*, e2416.

Ringstad, N., Gad, H., Low, P., Di, P. G., Brodin, L., Shupliakov, O., and De Camilli, P. (1999). Endophilin/SH3p4 is required for the transition from early to late stages in clathrin-mediated synaptic vesicle endocytosis. Neuron *24*, 143–154.

Schmid, E. M., and McMahon, H. T. (2007). Integrating molecular and network biology to decode endocytosis. Nature *448*, 883–888.

Sengar, A. S., Wang, W., Bishay, J., Cohen, S., and Egan, S. E. (1999). The EH and SH3 domain Ese proteins regulate endocytosis by linking to dynamin and Eps15. EMBO J. *18*, 1159–1171.

Soulet, F., Yarar, D., Leonard, M., and Schmid, S. L. (2005). SNX9 regulates dynamin assembly and is required for efficient clathrin-mediated endocytosis. Mol. Biol. Cell *16*, 2058–2067.

Stahelin, R. V., Long, F., Peter, B. J., Murray, D., De Camilli, P., McMahon, H. T., and Cho, W. (2003). Contrasting membrane interaction mechanisms of AP180 N-terminal homology (ANTH) and epsin N-terminal homology (ENTH) domains. J. Biol. Chem. *278*, 28993–28999.

Thomson, D. J. and Chave, A. D. (1991). Extraction of spots in biological images using multiscale products. In: Advances in Spectrum Analysis and Array Processing, ed. S. Haykin, Englewood Cliffs, NJ: Prentice Hall, 58–113.

Umeda, A., Meyerholz, A., and Ungewickell, E. (2000). Identification of the universal cofactor (auxilin 2) in clathrin coat dissociation. Eur. J. Cell Biol. *79*, 336–342.

Ungewickell, E., Ungewickell, H., Holstein, S. E., Lindner, R., Prasad, K., Barouch, W., Martin, B., Greene, L. E., and Eisenberg, E. (1995). Role of auxilin in uncoating clathrin-coated vesicles. Nature *378*, 632–635.

Ungewickell, E. J. and Hinrichsen, L. (2007). Endocytosis: clathrin-mediated membrane budding. Curr. Opin. Cell Biol. *19*, 417–425.

Wang, M. Q., Kim, W., Gao, G., Torrey, T. A., Morse, H. C., III, De, C. P., and Goff, S. P. (2003). Endophilins interact with Moloney murine leukemia virus Gag and modulate virion production. J. Biol. *3*, 4.

Wilbur, J. D., Chen, C. Y., Manalo, V., Hwang, P. K., Fletterick, R. J., and Brodsky, F. M. (2008). Actin binding by Hip1 (huntingtin-interacting protein 1) and Hip1R (Hip1-related protein) is regulated by clathrin light chain. J. Biol. Chem. *283*, 32870–32879.

Yamabhai, M., Hoffman, N. G., Hardison, N. L., McPherson, P. S., Castagnoli, L., Cesareni, G., and Kay, B. K. (1998). Intersectin, a novel adaptor protein with two Eps15 homology and five Src homology 3 domains. J. Biol. Chem. *273*, 31401–31407.

Yarar, D., Surka, M. C., Leonard, M. C., and Schmid, S. L. (2008). SNX9 activities are regulated by multiple phosphoinositides through both PX and BAR domains. Traffic *9*, 133–146.

Yarar, D., Waterman-Storer, C. M., and Schmid, S. L. (2005). A dynamic actin cytoskeleton functions at multiple stages of clathrin-mediated endocytosis. Mol. Biol. Cell *16*, 964–975.

Yarar, D., Waterman-Storer, C. M., and Schmid, S. L. (2007). SNX9 couples actin assembly to phosphoinositide signals and is required for membrane remodeling during endocytosis. Dev. Cell *13*, 43–56.

Zhang, C. X., Engqvist-Goldstein, A. E., Carreno, S., Owen, D. J., Smythe, E., and Drubin, D. G. (2005). Multiple roles for cyclin G-associated kinase in clathrin-mediated sorting events. Traffic *6*, 1103–1113.